Original Articles
cnj.araku.ac.ir

☑ Cite This: Colloid Nanosci. J. 3(2) (2025) 610-621 DOI: 10.61882/CNJ.3.2.610

Downregulation of NLRP3 by synthesized nanoencapsulated quercetin in human monocyte-like macrophages

Sepideh Moradkhani, Bita Fazel, Fatemeh Ayazi, Alireza Khosravi, Javad Malakootikhah, and Jalil Mehrzad*

Department of Microbiology and Immunology, Faculty of Veterinary Medicine, University of Tehran, Tehran, Iran

ARTICLE INFO

Article History:
Received 2025-09-05
Revised 2025-10-14
Accepted 2025-11-06

Corresponding Authors:
Jalil Mehrzad

Email:
mehrzad@ut.ac.ir

ABSTRACT

This study investigates the anti-inflammatory and pro-apoptotic properties of nanoencapsulated quercetin (QU) in a human monocyte-like macrophages (MLMs) model. Firstly, QU was purified using high-performance liquid chromatography (HPLC). Subsequently, the nanophytosome containing QU was prepared using the thin-film hydration method and its physicochemical properties were examined. Flow cytometry was conducted to analyze the apoptosis and necrosis of the MLMs. Also, gene expression of NOD-like receptor family pyrin domain-containing protein 3 (NLRP3) in MLMs was done by quantitative real-time PCR (qPCR). The HPLC analysis revealed a specific peak for QU at a retention time (RT) of 10.367 minutes. Moreover, the formulated nanoencapsulated QU, was with a size, polydispersity index (PDI), zeta potential, encapsulation efficiency (EE), loading capacity (LC) and 24-hour slow-release rate of <100 nm, ~0.3, -35.7 mV, 95%, 69% and 21.95%, respectively. Further, flow cytometry confirmed the remarkable increased apoptosis ($P< 0.0001$) in MLMs treated with nanoencapsulated QU. Gene expression by qPCR showed marked down-regulation of the key pro-inflammatory marker, NLRP3, at mRNA level. These findings highlight the potential of synthesized nanophytosome QU as an anti-inflammatory and apoptosis-inducing factor in human immune cells, and thus pharmacotherapy and biomedicine.

KEYWORDS: *Anti-inflammation, Apoptotosis, Human MLMs, Phytosome, NLRP3, Nanoencapsulated QU*

1. Introduction

Nanotechnology, as a novel science, was originally used for the recognition of flavonoids, such as quercetin, myricetin, rutin, and morin, compounds with antioxidant and anti-inflammatory activities [1, 2]. Quercetin (QU) is obtained from the Latin word *Quercetum*, meaning "oak tree" [3]. Quercetin, with the chemical formula C15H10O7, is a polyphenolic compound (3,3′,4′,5,7-pentahydroxyflavone), which is naturally found in leafy plants, fruits, vegetables, and shrubs [4-6]. Due to its poor water solubility, low chemical stability, and limited bioavailability, the practical application of QU in the food and pharmaceutical industries is restricted [7].

Phytosomes (phyto = plant, some = cell-like structure) are specifically designed to improve the absorption and bioavailability of plant-derived compounds, particularly poorly water-soluble drugs [8]. These nanostructures are formed as a result of stable interactions between phospholipids (mostly phosphatidylcholine) and polyphenolic phytochemicals [9, 10].

Phytosomes mainly increase encapsulation efficiency (EE), promote the chemical and biological stability of phytochemicals, facilitate their penetration across biological barriers, and intensify gastrointestinal absorption, thereby decreasing the required dose for a therapeutic effect and ultimately boosting therapeutic efficacy [11, 12].

QU has the immunomodulatory effects on several immune cell types, including macrophages (Mϕs) [13]. Functionally, Mϕs are divided into two chief phenotypes: classically activated Mϕs (M1), which principally mediate pro-inflammatory immune responses, and alternatively activated Mϕs (M2), which contribute to tissue repair and anti-inflammatory processes [14]. Moreover, human MLMs are cells differentiated from circulating monocytes that can develop into diverse Mϕs subsets, such as tissue-resident macrophages (TRMs) [15].

The *NLRP3* inflammasome has been widely studied as a key regulator of immune responses. This protein complex plays opposite roles in inducing inflammatory pathways and a pathogenic role in several autoinflammatory and autoimmune diseases; therefore, it emerges as a favorable therapeutic target for novel interferences [16]. However, limited studies evaluated the anti-inflammatory effects of nanophytosomal QU on NLRP3 activation in human MLMs.

The present study aimed to identify the safest and most effective dose of our synthesized nanoQU for modulating NLRP3 expression and apoptosis in human Mϕs. In addition, nanoencapsulated phytosomes were applied as the best drug delivery systems to improve the solubility, stability, and bioavailability of QU.

Therefore, following confirmation of QU purity by HPLC, the physicochemical properties of QU-loaded phytosomes were characterized. Further, EE%, LC%, and release kinetics of QU from the nanophytosomal QU structure were also determined. Subsequently, cultured MLMs were treated with different doses of nanoQU. Molecular techniques such as qPCR were employed to evaluate NLRP3 expression [17], while flow cytometry was used to assess apoptosis and necrosis [18]. Pharmacophysicochemically, our new formulated nanoQU would potentially be applicable as a valuable anti-inflammatory and apoptosis-inducing nanodrug in human, animal and biomedicine.

2. Materials and methods

2.1. Materials

Powdered and liquid soybean lecithin (phosphatidylcholine) (Titra Chem, Iran), ethanol, and phosphate-buffered saline (PBS) (Merck, Germany), quercetin anhydrous with a purity of >95% (Sigma-Aldrich, Germany), fetal bovine serum (FBS) (Gibco, USA), the complete Roswell Park Memorial Institute (RPMI)-1640 medium was supplemented with 2% human serum albumin, 2 mmol/L L-glutamine, 50 U/ml penicillin, 50 mg/ml streptomycin, FBS, kanamycin, gentamicin, non-essential amino acids, sodium pyruvate, and β-mercaptoethanol (2-ME). All reagents for RPMI preparation, except FBS, were purchased from Sigma-Aldrich. And ficoll was supplied by Biowest (France). Other chemicals and solvents used throughout the study were of analytical grade and applied in accordance with standard laboratory protocols.

2.2. Green synthesis of QU-loaded nanophytosomes and nanocapsules

Quercetin-loaded nanocapsules were prepared using the thin-film hydration method and sonication, according to standard protocols with varying molar ratios of QU and lecithin, as described in previous research [19]. In brief, almost 60 mg of lecithin was dissolved in 6 mL of ethanol, and 30 mg of QU was dissolved in 2 mL of ethanol. The combined solution was transferred into a round-bottom flask, and solvent evaporation was performed under vacuum at 60 °C for 60 minutes at 1300 rpm, forming a thin lipid film on the flask wall. After 10 mL of distilled water was added, hydration was attained using a rotary evaporator (without vacuum) for 30 minutes at 68 °C. Lastly, the particle size of the nanophytosomes was reduced by probe sonication [20].

2.3. Physicochemical characterization of QU-loaded nanocapsules

The physicochemical properties of QU-loaded nanocapsules were assessed using numerous analytical techniques. First, the purity of QU was confirmed by HPLC (Knauer, Germany) through comparison with a reference standard [21]. The morphology and exact particle size of the QU-loaded nanocapsules were then assessed using scanning electron microscopy (SEM). Further, the EE%, LC% of QU within the phytosomes, and the controlled release profile of the active compound were set according to the established protocols with minor modifications [22]. Eventually, particle size, PDI, and zeta potential of the QU nanocapsules were measured using a Zetasizer system based on dynamic light scattering (DLS) (Malvern Zeta-Sizer Nano-ZS, UK).

2.4. Confirmation of QU purity by optimized HPLC

The pure QU was approved using an optimized HPLC method. Mobile phase composition, pH, column characteristics, flow rate, and detection wavelength were adjusted. The ultimate mobile phase (700:300:1, v/v/v, methanol, distilled water, and trifluoroacetic acid) was delivered by a KNAUER dual reciprocating pump (Model K-1001) at a flow rate of 0.8 ml/min. The detected peaks at 254 nm were isolated on an Inertsil C18 column (150 × 4.6 mm, 5 µm particle size) during a 20-minute run time. A 20 µL sample was injected using a Rheodyne injector (PerkinElmer, Waltham, MA, USA), and the retention time (RT) for QU was 10.36 minutes. Additionally, blank and standard solutions were used in the injection sequence for certifying analytical accuracy.

2.5. Encapsulation Efficiency and LC% of QU in phytosomes

To reduce particle size, multilayered nanoencapsulated particles were subjected to sonication using a probe sonicator (Dr. Hielscher, Germany) for 20 minutes with 1-minute intervals to prevent overheating, under controlled cold conditions (4-6 °C). The resulting suspension was passed through a 0.22 µm filter (Gibco, USA) to improve structural uniformity and enhance physicochemical stability of the final product. Free QU was detached using a dialysis bag with a 10 kDa molecular weight cutoff, dipped in PBS at 4 °C for 2 hours with gentle stirring. For determination of EE% and LC%, the filtered suspension was diluted with 96% ethanol at ratios of 1:2, 1:5, and 1:10, and absorbance was measured at 370 nm using a UV/VIS spectrophotometer (Pharmacia Novaspec II, Germany). Results were compared against a QU calibration curve ($y = 0.0018x + 0.081$, $R^2 = 0.9956$). At last, EE% and LC% were calculated under standard formulas with minor modifications [23].

$$EE\% = \frac{Total\ amount\ of\ QU\ (mg) - amount\ of\ QU\ in\ precipitate\ (mg)}{Total\ amount\ of\ QU\ (mg)} \times 100$$

Eq. (A.1)

$$LC\% = \frac{Total\ amount\ of\ QU\ (mg) - amount\ of\ QU\ in\ precipitate\ (mg)}{Total\ amount\ of\ phytosome\ (mg)} \times 100$$

Eq. (A.2)

Evaluation of QU release kinetics from phytosomes under simulated gastric conditions regarding the dialysis bag diffusion method, 1 mL of suspension was placed into a dialysis bag and dipped in 10 mL of PBS (pH 4.5) at 37 °C under continuous stirring. At specified intervals (0.5, 1, 2, 4, 6, and 24 hours), 1 mL of the release medium was removed and replaced with an equal volume of fresh buffer. The optical density was measured at 370 nm. Data from three replicates were reported as mean ± standard error of means (sem). The release kinetics of QU from the phytosome exhibited a gradual and steady release under gastric conditions.

2.6. Study population and sampling method

In the present study, 6 healthy human volunteers (20-30 years, matched gender, with no history of underlying disease) were enrolled as donors of MLMs. Participants were randomly put into two groups: a control group (untreated MLMs) and a treatment group (nanoencapsulated QU-treated MLMs). In general, considering the variable molecule (NLRP3) and to increase predictive accuracy, all selected young healthy participants were free from any diseases and abnormalities. Based on previous studies, we tested various doses of nanoQU (QU itself have been very safe, preliminarily tested on human peripheral blood mononuclear cells (PBMCs) flow cytometrically) a concentration of 6 mg/mL of the nanoQU (dilution ratios 1:50 [as the optimal dose] was tested to determine the safest and most effective dose [24]. Informed consent was obtained from all volunteers following a full explanation of the study protocol. Heparinized blood samples were collected under sterile conditions using a simple sampling method and diluted at a 1:1 ratio with PBS. The samples were then transferred to the central laboratory of the Faculty of Veterinary Medicine, University of Tehran, for subsequent cell isolation and experimental measurements.

2.7. Isolation and culture of MLMs

The current study was approved by the Ethics Committee of the Faculty of Veterinary Medicine, University of Tehran, under the ethical number of IR.UT.VETMED.REC.1403.016. The PBMCs were separated as previously reported with minor modifications [18]. Briefly, 15 mL of blood samples were diluted (1:1) with PBS and carefully poured over 15 mL of Ficoll. Then, samples were

centrifuged (800 ×g, 18 °C, 45 min), yielding PBMCs, and the collected cells were washed once with PBS (750 ×g, 4 °C, 10 min) and twice with complete RPMI-1640 medium containing 10% FBS, 1% penicillin/streptomycin (P/S), 1% kanamycin, and 1% gentamicin (450 ×g, 4 °C, 5 min each). The viability of the cells reached>98% by this protocol. About 1×10^7 PBMCs/mL were seeded in culture plates (incubated for 2 h at 37 °C in 95% humidity and 5% CO_2). From isolated PBMCs, the monocytes were separated based on a technique involving in their plastic adherence properties [25]. The quality and viability of MLMs were also counted and checked using a microscopical hemocytometer [26, 27]. Non-adherent cells were removed from isolated PBMCs by washing with RPMI. Afterward, adherent cells, which were confirmed as almost pure monocytes by eosin–Giemsa staining [26], and subsequently these adhered cells (i.e., highly pure monocytes) were collected and cultured for an additional 24 h to have MLMs (see representative figure in the result section). Then, these cells were transferred in RPMI-1640 medium containing 100 U/mL penicillin, 100 µg/mL gentamicin, and 0.3 mg/mL L-glutamine for subsequent experiments. Generally, 4×10^6 MLMs/mL were seeded in 12-well plates and treated with 6 mg/mL nanoencapsulated QU (containing 60 µM QU) as an optimized dose for 24 h. The MLMs particularly were then either freshly used for flow cytometry assays or were kept at -80 °C for qPCR assays.

2.8. Evaluation of apoptosis and necrosis in MLMs using flow cytometry

With Annexin V/Propidium Iodide (PI), the evaluation of MLMs death was analyzed by flow cytometry, following simultaneous staining with PI and Annexin V labelled with fuorescein isothiocyanate (FITC), using the Annexin V-FITC Apoptosis Detection Kit (BioLegend, Cat #:640914). The externalization of phosphatidylserine as a marker of early-stage apoptosis was detected by the Annexin V protein conjugated to FITC, whereas membrane damage due to late stage apoptosis/necrosis was detected by the binding of PI to nuclear DNA. Briefly, 1×10^6 MLMs were exposed to a defined concentration of nanoQU for 24 h at 37 °C. Later, MLMs were centrifuged, and 100 µL of fresh MLMs suspension was incubated with 1.3 µL Annexin V-FITC in 140 µL binding buffer (provided in the kit) for 20 min at 4 °C. Two groups of unstained and single-color controls, consisting of either 0.5 µL PI or 1.3 µL Annexin V-FITC, were incorporated to set compensation and gating parameters [18]. Next, 140 µL of 1x binding buffer was added to each sample, and after washing, Annexin V-FITC/PI staining was analyzed using flow cytometry. Briefly, samples were analyzed in an Accuri C6 flow cytometer [BD FACS Calibur (BD biosciences, San Jose, CA, USA)]. For the data analyses, the wavelength for Annexin V-FITC (FL1-H) and PI (FL2-H and FL3-H) was set at 520nm and 617nm, respectively, and fluorescence signals, for at least 10000 events for each sample, were counted in a numerical and logarithmic mode and the data were finally analyzed using FlowJo Version 10.10 (Accuri) software. To quantitatively assess the fraction of apoptotic cells, the Annexin V-FITC apoptosis detection kit was used with flow cytometry. The flow cytometry-based MLMs staining with both Annexin V-FITC and PI was carried out according to the Annexin V-FITC kit's manufacturer's protocol. Briefly, the MLMs were washed with PBS and resuspended in 100 µl of ×1 binding buffer. Subsequently, 5 µl of FITC-conjugated Annexin V-FITC was added, and the mixture was incubated at room temperature in the dark for 10 min, then washed and the supernatants were removed, addition of of PI staining solution, cells were incubated for 10 min at room temperature in the dark. The MLMs were analyzed using the FACS Calibur flow cytometry with a range emission filters set to 515–545 nm for FITC (green) and ~600 nm for PI (red). Data analyses were performed using Cell Quest software (Becton Dickinson, Mountain View, CA) that segmented the two-dimensional Annexin V-FITC versus PI staining into four quadrants (Q), where Q1, Q2, Q3 and Q4 represents necrotic, late apoptotic, early apoptotic and viable MLMs, respectively. The flow cytometry experiments were carried and repeated independently at least 4 times.

2.9. Measurement of NLRP3 expression in human MLMs using qPCR

At first, total ribonucleic acid (RNA) was extracted from 1×10^6 cells using a commercial extraction reagent (Biotech, China), dissolved in nuclease-free water (Promega, USA), and stored at -80 °C until further analysis. Ribonucleic acid concentration and purity were measured using a NanoDrop 2000 spectrophotometer (Boeco, Germany), and integrity was confirmed by gel electrophoresis. For complementary DNA (cDNA)

Table 1. Detailed description of designed primers used for mRNA expression of NLRP3 in human monocyte-like macrophages.

Gene	Sequence (5′ to 3′)	Size (bp)	Annealing (°C)
GAPDH	F: CGCTCCTGGAAGATGGTGATGG R: GTATTGGGCGCCTGGTCACC	158	56
NLRP3	F: GGACTGAAGCACCTGTTGTGCA R: TCCTGAGTCTCCCAAGGCATTC	153	56

synthesis, 0.5-1 µg of RNA from each sample was exposed to reverse transcriptase (RT) reactions with 50 µg of oligo(dT) primers using a cDNA synthesis kit (Yektatajhiz, Iran). Glyceraldehyde 3-phosphate dehydrogenase (GAPDH) was used as the internal housekeeping control. A final volume of 10 µL qPCR reaction was produced containing 0.25 µL of each forward and reverse primer, 5 µL of 2× SYBR Green Master Mix (YTA, Iran), and 0.25 µL of cDNA template and 4.5µL nuclease free water. Amplification was performed using a CFX Connect™ Real-Time PCR system (QIAGEN, Germany). To establish amplification efficiency, a series of 10-fold serial dilutions of cDNA was prepared. All primers were checked for the position and extra bands using Beacon Designer v8, Oligo, and NCBI, Primer-BLAST, and they were diluted and used according to the manufacturer's protocol. Detailed description of the designed primers used for qPCR are available in Table 1.

The triplicate qPCR reactions had specific thermal cycling conditions that were made up of an initial holding at 95 °C for 10 min, 40 cycles of denaturation at 95 °C for 10 s, annealing at 53-62 °C with an average of 55 °C for 20 s, and extension at 72 °C for 25 s. Fluorescence signals were registered at the end of each extension phase. A single obvious peak of the melt curve from 52 °C to 95 °C with 1 °C augmentation (5 s per step), affirming the specificity of amplification. Additionally, agarose gel electrophoresis was used to certify the qPCR product. Data were analyzed using REST software (QIAGEN). The crossing point (CP) values were arranged for each replicate, and the mean CP values were calculated across six biological replicates. Relative gene expression was estimated using ΔΔCt methods as previously done [17, 18, 25]. Data was analyzed to determine fold changes in target gene (NLRP3) using the comparative threshold cycle (Ct) method, calculating $2^{-\Delta\Delta Ct}$. The fold change, or $2^{-\Delta\Delta Ct}$, was determined by normalizing the Ct of the target gene relative to the related reference gene (GAPDH) in both control and nanoQU-treated groups. The ΔCt for treated genes was normalized to the calibrator, calculated as ΔΔCt = ΔCt (treated) – ΔCt (calibrator). Finally, the relative gene expression fold change was expressed as fold change = $2^{-\Delta\Delta Ct}$. After normalization, these values for treated samples were transformed to a natural logarithm (Ln) scale for clearer presentation [17, 18, 25]. The resulting qRT-PCR data are presented as mean ± sem for 6 samples.

2.10. Statistical Analysis

The statistical analyses were done by GraphPad Prism 10 (GraphPad Software Inc., California, USA). Apart from normalizing the results of qPCR for gene expression data of NLRP3, which was normalized against GAPDH expression, and mean fluorescence intensity (MFI) values gained for apoptosis and necrosis analyses, the descriptive statistics described and presented as mean ± sem. The comparison between 2 groups (i.e., control group (untreated MLMs) and a treatment group (nanoQU-treated MLMs) was done by independent *t*-test. A P-value of ≤ 0.05 was reflected as statistically significant.

3. Results and Discussion

3.1. HPLC analysis and physicochemical characteristics of nanoencapsulated QU

The chromatogram of the diluted control sample showed no interfering peaks, whereas the QU standard indicated a sharp and well-defined peak with different properties (Fig. 1).

The HPLC method in the present study revealed high selectivity and specificity, which can provide the effective isolation of QU during chromatographic analysis. In similar research aimed at measuring QU in rat samples, a novel HPLC technique was set using a Supelcosil LC-18T C18 column and an isocratic mobile phase consisting of 0.3% trichloroacetic acid in water and acetonitrile (50:50, v/v), a flow rate of 0.9 mL/min for a run-time of 13 minutes. The detection wavelength was 254 nm [28]. However, another

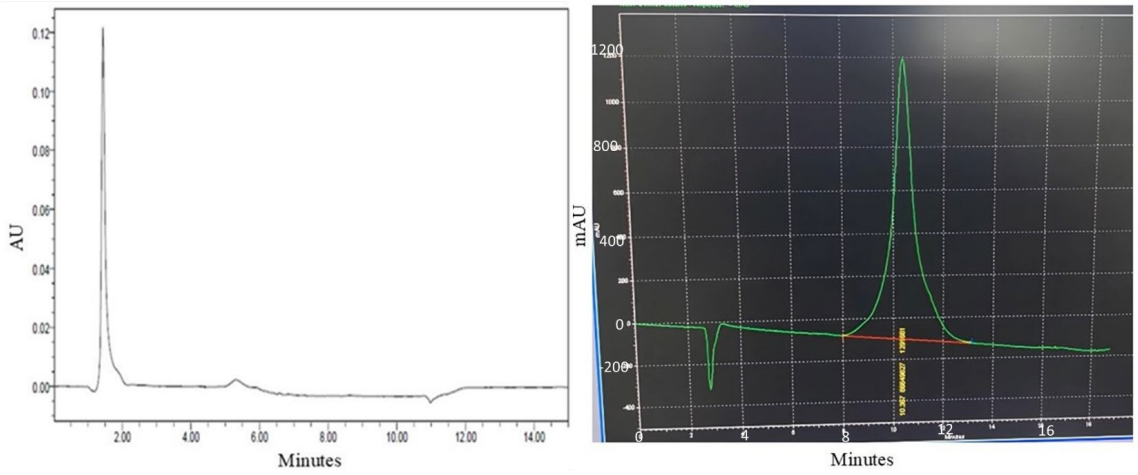

Fig. 1. High-performance liquid chromatography (HPLC) chromatogram characteristics for the assessment of quercetin (QU) purity. (Left) blank diluent sample demonstrating no specific peak**(s)**, confirming method selectivity without interference. (Right) chromatogram of the QU standard, with a sharp peak at a retention time (RT) of 10.367 minutes, peak area of 86,649,627, and peak height of 1,291,661 highlighting high purity (above 95%) with slight impurities visible as a smaller peak preceding the main peak.

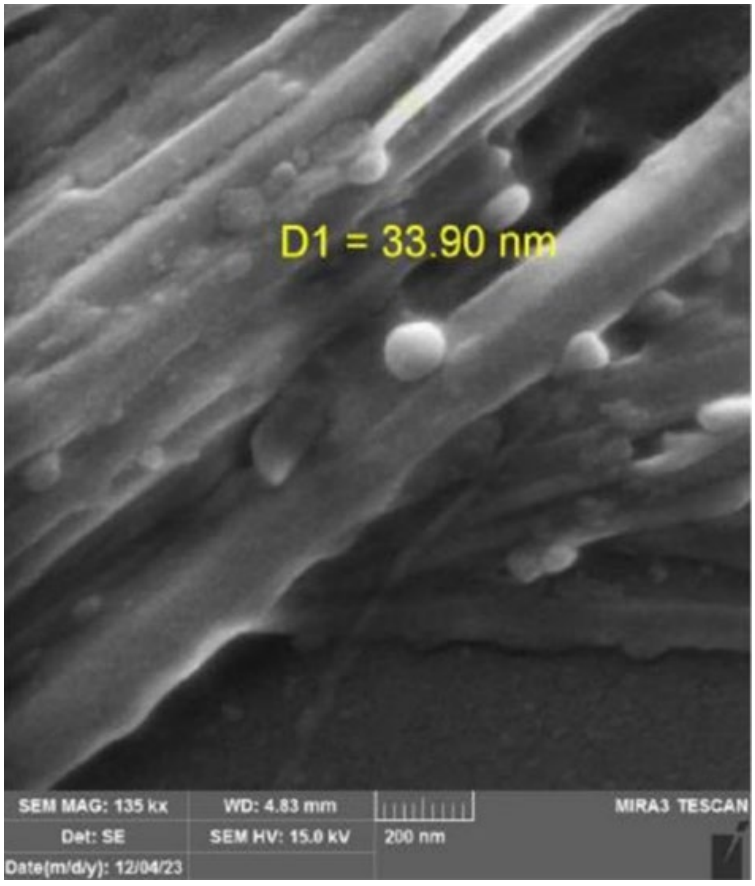

Fig. 2. Scanning Electron Microscopy (SEM) pictures of nanoencapsulated QU particles. The very closer view of the image depicts the overall distribution and morphology of the synthesized nanoquercetin, emphasizing an individual nanoparticle with a diameter of 33.90 nm, thus verifying the nanoscale size of the formulation.

study in 2023 optimized the HPLC extraction method of QU based on the detection wavelengths of 210 and 347 nm [29]. These findings emphasize that the choice of column type, mobile phase, and detection wavelength significantly affects the sensitivity and accuracy of QU quantification.

Scanning Electron Microscopy images illustrated two distinguished structural patterns within the QU-loaded nanocapsules. The first one consisted of fibrous strands, probably resulting from the incomplete solubility of lecithin during the phytosome preparation process. The second one was composed of uniformly diffused spherical particles, with the smallest particle size of 33.90 nm in diameter (Fig. 2). The particle size of <100 nm was in agreement with the findings of DLS analysis. Research in 2021 also reported particle sizes of <100 nm for QU nanocapsules [30]. These results support the improved applications of nanoscale QU nanocapsules with a consistent size distribution in the biomedical and pharmaceutical industries.

The QU calibration curve and calculation formulas demonstrated that the EE% and drug LC% were 95% and 69%, respectively. These findings support the potential of nanophytosomes as a proper delivery system for bioactive compounds such as QU. Additionally, the ultrasound not only reduces particle size but also increases the surface area of phytosomes. Moreover, it enhances the amount of active composite associated with phospholipid membranes, which in turn refines drug LC. The results are consistent with previous investigations on phosphatidylcholine-based complexes, such as Rutin, which exhibited an EE% above 90% [31]. In a recent evaluation of vitamin C-loaded chitosan-coated nanoliposomes, LC% was reported 50.67% ± 1.12, which was lower than the expected value in the present study [32]. Furthermore, drug release evaluation under simulated gastric conditions (pH 4.5, 37 °C) showed a rapid initial release during the first six hours, followed by a sustained release phase. After 24 hours, the cumulative release reached 21.95% ± 0.001 (data not shown). A likely explanation for the reduced release rate is the ionization of carbonyl groups within the phytosome structure under acidic conditions (pH 4.5), which increases capsule stability. In agreement with these findings, a study on chia seed oil microencapsulation using nanoliposomes also expressed a sustained release pattern under acidic conditions [33].

Our DLS analysis displayed that the mean size of our synthesized nanoQU was 58.93 nm, with a PDI of 0.34, reflecting a relatively uniform size distribution (Fig. 3A). Since the PDI values of all samples were below 0.5, the nanoparticles manifested a uniform size distribution. According to a report, nanophytosomes which possess cumin essential oil, prepared by the thin-film hydration-sonication method, presented particle sizes of <100 nm and a PDI of <0.3 [30]. In addition, the measured zeta potential was −35.7 mV (Fig. 3B). The negative surface charge of the nanoparticles, allocated to the presence of negatively charged functional groups during their synthesis, allowed electrostatic repulsion forces that effectively inhibited particle aggregation and contributed to the stability of the nanocapsule system. A similar study conducted in 2023 reported the zeta potential of QU nanocapsules prepared using the thin-film hydration method as −35.93 ± 0.95 mV [34], which is in line with our current findings.

3.2. Effects of nanoencapsulated QU on apoptosis, cell survival, and NLRP3 gene expression in MLMs

To evaluate the effects of nanoencapsulated QU on the survival and NLRP3 gene expression of MLMs, 10^4 cells were analyzed. The results revealed that treatment with NanoQU exerted little effects on cellular necrosis, i.e., lower necrotic MLMs in NanoQU-treated group (P=0.0002); (Fig. 4A). However, a significant increase in early and late apoptosis was observed at lower concentrations of NanoQU compared to the untreated group (P=0.0002 and P<0.0001 respectively) (Fig. 4A). In similar studies, while the effect of NanoQU treatment on cellular necrosis has generally been reported as minor, a significant increase in apoptosis was observed at such low doses of QU-loaded nanocapsules. For example, researchers [35] designed a polymeric nanocapsule co-loaded with docetaxel (DTX) and QU for targeted prostate cancer therapy, reporting enhanced apoptotic induction and a significant reduction in tumor growth in *in-vivo* models.

In addition, as shown in Fig. 4B, the results, including an amplification curve of the GAPDH and NLRP3 genes based on cycle threshold (Ct) values and melt curve analysis based on the natural logarithm of fold change (lnFC) further confirmed the accuracy and reliability of the qPCR assay used

in the current study. Besides, NanoQU treatment led to a noticeable lowering in the inflammatory NLRP3 gene expression using the qPCR technique (P< 0.0001) (Fig. 4B). Activation of the NLRP3 inflammasome is recognized as a central mechanism in the pathogenesis of severe systemic inflammatory conditions, often referred to as cytokine storm [36] or cytokine release syndrome. This molecular complex plays a crucial role in triggering a broad spectrum of inflammatory mediators. Compatible with the findings of the current study, both *in-vitro* and *in-vivo* studies have proved that QU can efficiently inhibit NLRP3 inflammasome activation, thereby highlighting its potential as a promising therapeutic agent for preventing excessive inflammatory responses [37, 38].

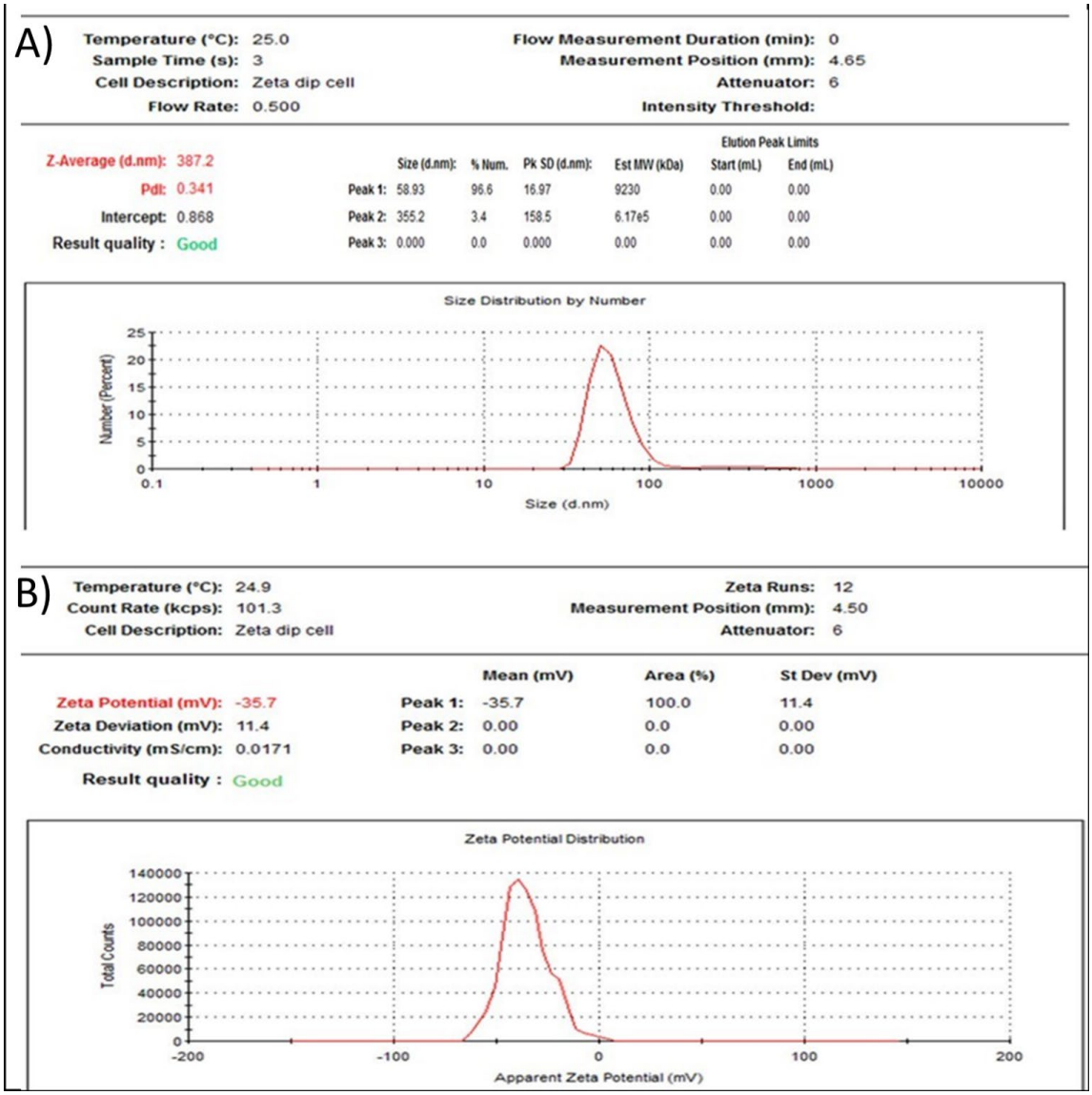

Fig. 3. Dynamic light scattering (DLS) and zeta potential distribution of the nanoencapsulated Quercetin (QU). **(A)** illustrates a sharp peak with the mean particle size of 58.93 nm with the polydispersity index (PDI) of 0.34. The analysis was conducted at 25°C and the intercept of the sample was 0.868. **(B)** depicts a sharp peak at -35.7 mV. The analysis was done at 24.9°C with a mean deviation of 11.4 mV. The conductivity of the sample was measured at 0.0171 millisiemens/centimeter (mS/cm).

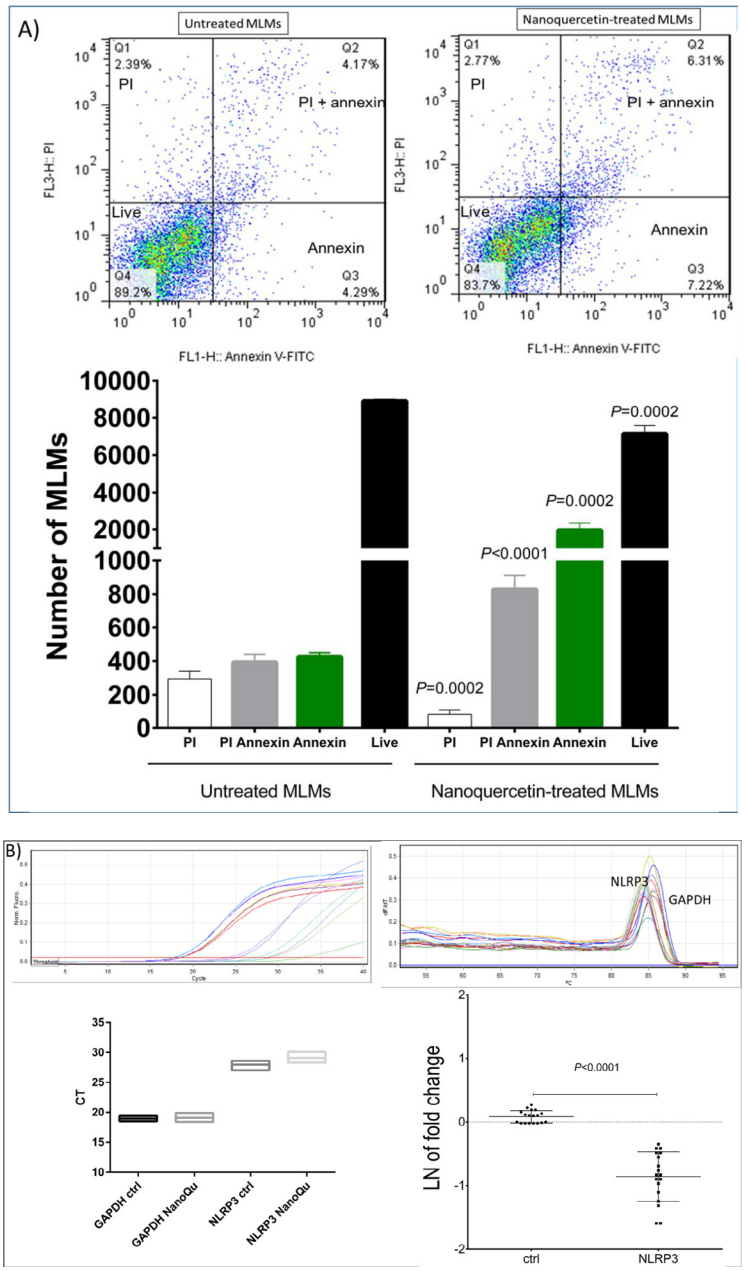

Fig. 4. Effects of nanoencapsulated Quercetin (nanoQU) on apoptosis, necrosis **(A)**, and NLRP3 Gene Expression **(B)** in MLMs. Dot plots and fold-change analyses were created to assess apoptosis, necrosis, and NLRP3 gene expression in monocyte-like macrophages (MLMs). The upper part of panel A representatively depicts flow cytometry profiles of untreated and nanoQU-treated MLMs. The four quadrants of each plot clearly show live cells (lower left), necrotic cells (upper left), early apoptotic cells (lower right), and late apoptotic cells (upper right). The lower part of panel A illustrates histogram data summarizing cell counts in each quadrant, with a significantly increased number of early and late apoptotic cells (P= 0.0002 and P< 0.0001, respectively). In panel B, the upper left and upper right representatively show the amplification curve based on cycle threshold (Ct) values and the melting curve, respectively, of the NLRP3 and GAPDH genes, confirming efficient and reproducible amplification with consistent exponential phases and single melting peaks without nonspecific amplification or primer-dimer formation for NLRP3 and GAPDH genes. The lower left and lower right of panel B are Ct values and analyzed overall mRNA expression of NLRP3 (based on the natural logarithm of fold change (lnFC) in NanoQU-treated MLMs. The fold change curve shows a significant reduction in NLRP3 inflammatory gene expression following naanoQU treatment in MLMs (P < 0.0001). Data are stated as mean ± SED from four (n=4) and six (n=6) independent replicates for flow cytometry and qPCR, respectively.

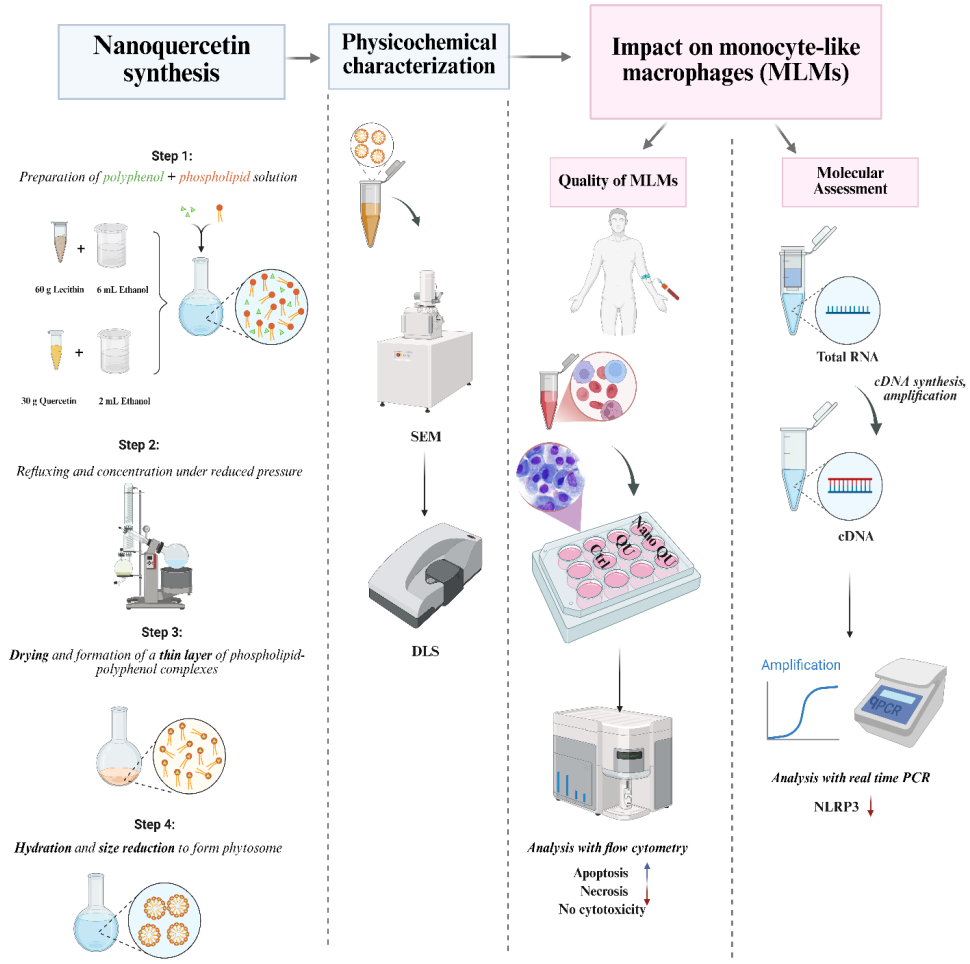

Fig. 5. The schematic process of physicochemically acceptable nanoencapsulated quercetin (nanoQU) preparation, along with its physicochemical characteristics and anti-inflammatory-and-safely anti-necrotic impacts on human's key immune cells, *i.e.,* highly differentiated monocyte, with downregulation of MLMs' key pro-inflammatory molecules, NLRP3.

Overall finding of the current study is schematically depicted in figure 5; as seen, we synthesized pharmacophysicochemically-and clinically relevant nanoQU that possesses anti-inflammatory activities in one of human's key immune cells, MLMs, which could be suitable for biomedical application. Indeed, the synthesized nanoQu are safely applicable as new anti-inflammatory compounds as pharmacotherapy in human and animals.

4. Conclusion

The practical use of QU in the food and pharmaceutical industries is limited because of several reasons such as its poor water solubility, little chemical stability, and restricted bioavailability. So, nanophytosomes, as progressive drug delivery nanocapsules, are applied to increase the solubility, stability, and bioavailability of QU. The present study intended for identifying the safest and most effective dose of nanoQU for regulating NLRP3 expression and apoptosis in human Mϕs. In brief, QU nanophytosomes were successfully prepared using a green and thin-film hydration–sonication method. The nanocapsules demonstrated a high EE% (95%), a LC% of 69%, and a sustained, controlled drug release profile, confirming their potential as a competent drug delivery system. As well, physicochemical properties assessment through HPLC, SEM, and DLS confirmed the

formation of spherical nanoparticles, which had a mean size of 58.93 nm with a PDI of 0.34, and a zeta potential of -35.7 mV. The synthesized nanoQU also significantly caused the low expression of the pro-inflammatory gene NLRP3 in key immune cells. These findings verify a critical role of our nanoQU as a promising therapeutic candidate for the prevention and treatment of various inflammatory disorders in human and animals.

Conflicts of Interest

The authors declare that they have no known competing financial interests or personal relationships that could have affected the work reported in this paper.

Acknowledgments

The present study was conducted as part of a Ph.D. dissertation in Immunology at the Faculty of Veterinary Medicine, University of Tehran, on healthy student volunteers of this faculty. Special cellular and molecular diagnostic tests were performed at the Central Laboratory of the Faculty of Veterinary Medicine. Part of the preparation process and related assays of nanoencapsulated QU were done at the Faculty of Chemistry, University of Tehran, and Mabna Diagnostic Laboratory, Tehran. The authors sincerely appreciate the employees of these Diagnostic Laboratories for their precious support and assistance.

References

[1] O. Lozano, A. Lazaro-Alfaro, C. Silva-Platas, Y. Oropeza-Almazan, A. Torres-Quintanilla, J. Bernal-Ramirez et al., Nanoencapsulated Quercetin Improves Cardioprotection during Hypoxia-Reoxygenation Injury through Preservation of Mitochondrial Function, Oxid Med Cell Longev. 2019 (2019) 7683051. https://doi.org/10.1155/2019/7683051

[2] A. Gomes, E. Fernandes, J.L. Lima, L. Mira, M.L. Corvo, Molecular mechanisms of anti-inflammatory activity mediated by flavonoids, Curr Med Chem. 15 (2008) 1586–605. https://doi.org/10.2174/092986708784911579

[3] F. Aghababaei, M. Hadidi, Recent Advances in Potential Health Benefits of Quercetin, Pharm. 16 (2023) 1020. https://doi.org/10.3390/ph16071020

[4] C. Zhou, Y. Lin, Osteogenic differentiation of adipose-derived stem cells promoted by quercetin, Cell Prolif. 47 (2014) 124–132. https://doi.org/10.1111/cpr.12097

[5] A. Ch. Pradyutha, S. Yadam, R. V. Umamaheswara, In vitro antioxidant activity, antidiabetic activity and in silico docking studies of 3,3',4',5,7-pentahydroxyflavone and stigmasta-5,22-dien-3β-ol isolated from aerial parts of Euphorbia milii, Des moul. Nat Prod Res. 39 (2025) 2695–2702. https://doi.org/10.1080/14786419.2024.2307998

[6] E.J. Carrillo-Martinez, F.Y. Flores-Hernandez, A.M. Salazar-Montes, H.F. Nario-Chaidez, L.D. Hernandez-Ortega, Quercetin, a Flavonoid with Great Pharmacological Capacity, Molecules. 29 (2024) 1000. https://doi.org/10.3390/molecules29051000

[7] H. Joshi, D.S. Gupta, G. Kaur, T. Singh, S. Ramniwas, K. Sak et al., Nanoformulations of quercetin for controlled delivery: a review of preclinical anticancer studies, N-S Arch Pharmacol. 396 (2023) 3443–3458. https://doi.org/10.1007/s00210-023-02625-z

[8] S. Sharma, N. Gupta, Review on phytosomes: as an emerging strategy to improve the bioavailability of phytoconstituents, Am J PharmTech Res. 10 (2020): 121–134. ISSN: 2249-3387

[9] H.A. Pawar, B.D. Bhangale, Phytosome as a novel biomedicine: a microencapsulated drug delivery system, JBABM. (2015) 7. https://doi.org/10.4172/1948-593X.1000116

[10] J. Dwivedi, P. Wal, S. Kaushal, A.K. Tripathi, P. Gupta, S.P. Rao, Phytosome-based cosmeceuticals for enhancing percutaneous absorption and delivery, J. Res. Pharm. 29 (2025) 242–271. https://doi.org/10.12991/jrespharm.1643734

[11] M. Saritha, A. Ramya, A. Sonia, S. Monika, K. Sowmya, Phytosomes: A Novel approach for improving the efficacy of Herbal Extracts, RJPT. 16 (2023) 6028–6031. https://doi.org/10.52711/0974-360X.2023.00978

[12] M. Barani, E. Sangiovanni, M. Angarano, M.A. Rajizadeh, M. Mehrabani, S. Piazza et al., Phytosomes as innovative delivery systems for phytochemicals: A comprehensive review of literature, Int J Nanomedicine. (2021): 6983–7022. https://doi.org/10.2147/IJN.S318416

[13] L. An, Q. Zhai, K. Tao, Y. Xiong, W. Ou, Z. Yu et al., Quercetin induces itaconic acid-mediated M1/M2 alveolar macrophages polarization in respiratory syncytial virus infection, Phytomedicine. 130 (2024): 155761. https://doi.org/10.1016/j.phymed.2024.155761

[14] S. Epelman, K.J. Lavine, G.J. Randolph, Origin and functions of tissue macrophages, Immunity. 41 (2014) 21–35. http://dx.doi.org/10.1016/j.immuni.2014.06.013

[15] A. Saradna, D.C. Do, S. Kumar, Q.L. Fu, P. Gao, Macrophage polarization and allergic asthma, Transl Res. 191 (2018):1–14. https://doi.org/10.1016/j.trsl.2017.09.002

[16] C. Napodano, V. Carnazzo, V. Basile, K. Pocino, A. Stefanile, S. Gallucci et al., NLRP3 inflammasome involvement in heart, liver, and lung diseases—a lesson from cytokine storm syndrome, Int J Mol Sci. 24 (2023): 16556. https://doi.org/10.3390/ijms242316556

[17] J. Mehrzad, A.M. Malvandi, M. Alipour, S. Hosseinkhani, Environmentally relevant level of aflatoxin B1 elicits toxic pro-inflammatory response in murine CNS-derived cells, Toxicol Lett. 279 (2017) 96–106. https://doi.org/10.1016/j.toxlet.2017.07.902

[18] J. Mehrzad, A. Bahari, M.R. Bassami, M. Mahmoudi, Dehghani H. Immunobiologically relevant level of aflatoxin B1 alters transcription of key functional immune genes, phagocytosis and survival of human dendritic cells, Immunol Lett. 197 (2018) 44–52. https://doi.org/10.1016/j.imlet.2018.03.008

[19] W. Maryana, H. Rachmawati, D. Mudhakir, Formation of phytosome containing silymarin using thin layer hydration technique aimed for oral delivery, Mater

Today Proc. 3 (2016) 855–866. https://doi.org/10.1016/j.matpr.2016.02.019

[20] B. Ghanbarzadeh, A. Babazadeh, H. Hamishehkar, Nanophytosome as a potential food-grade delivery system. Food bioscience. 15 (2016) 126–135. https://doi.org/10.1016/j.fbio.2016.07.006

[21] P.M. D'Mello, U.J. Joshi, P.P. Shetgiri, T.K. Dasgupta, K.K. Darji, A simple HPLC method for quantitation of quercetin in herbal extracts, J. AOAC Int. 94 (2011) 100–105. https://doi.org/10.1093/jaoac/94.1.100

[22] M. Mohammadpanah, E. Mojodi, F. Haghiralsadat, S.K. Sabbagh, M. Rajabi, Lavandula Angustifolia Essential Oil Loaded in Liposomal Nano-Carriers Regulate the HER2 and CASP3 Genes in MCF-7 and SK-BR-3 Cell-Lines, Res Sq. (2020) 1-20. https://doi.org/10.21203/rs.3.rs-40618/v1

[23] H. Moon, P. Lertpatipanpong, Y. Hong, C.T. Kim, S.J. Baek, Nano-encapsulated quercetin by soluble soybean polysaccharide/chitosan enhances anti-cancer, anti-inflammatory, and anti-oxidant activities, J. Funct. Foods. 87 (2021) 104756. https://doi.org/10.1016/j.jff.2021.104756

[24] J. Li, Z. Sun, G. Luo, S. Wang, H. Cui, Z. Yao et al., Quercetin attenuates trauma-induced heterotopic ossification by tuning immune cell infiltration and related inflammatory insult, Front Immunol. 12 (2021) 649285. https://doi.org/10.3389/fimmu.2021.649285

[25] Z. Karami, J. Mehrzad, M. Akrami, S. Hosseinkhani, Anti-inflammation-based treatment of atherosclerosis using Gliclazide-loaded biomimetic nanoghosts, Sci Rep. 13 (2023) 13880. https://doi.org/10.1038/s41598-023-41136-y

[26] A. Mohammadi, J. Mehrzad, M. Mahmoudi, M. Schneider, A. Haghparast, Effect of culture and maturation on human monocyte-derived dendritic cell surface markers, necrosis and antigen binding, Biotech Histochem. 90 (2015) 445–452. https://doi.org/10.3109/10520295.2015.1017536

[27] S. Kamiloglu, G. Sari, T. Ozdal, E. Capanoglu, Guidelines for cell viability assays, Food Front. 1 (2020) 332–349. https://doi.org/10.1002/fft2.44

[28] K.S. Abdelkawy, M.E. Balyshev, F. Elbarbry, A new validated HPLC method for the determination of quercetin: Application to study pharmacokinetics in rats, Biomed Chromatogr. 31 (2017) e3819. https://doi.org/10.1002/bmc.3819

[29] L.Q. Li, J. Cheng, F. Lu, Y.D. Du, Y. Xie, C. Zhou et al. Optimized HPLC extraction method of quercetin and berberine based on response surface analysis, RSC Advances. 13 (2023) 29427-29437. https://doi.org/10.1039/D3RA04384C

[30] M. Mohammadi, H. Hamishehkar, M.K. Piruzifard, Nanophytosome as a promising carrier for improving cumin essential oil properties, Food Biosci. 42 (2021) 101079. https://doi.org/10.1016/j.fbio.2021.101079

[31] A. Babazadeh, B. Ghanbarzadeh, H. Hamishehkar, Phosphatidylcholine-rutin complex as a potential nanocarrier for food applications, J. Funct Foods. 33 (2017) 134–141. https://doi.org/10.1016/j.jff.2017.03.038

[32] A. Salimi, B. Sharif-Makhmalzadeh, M. Salahshoori, Preparation and in-vitro Evaluation of Protective Effects of Quercetin-Loaded Solid Lipid Nanoparticles on Human Hair Against UV-B Radiation, J. Cosmet. Dermatol. 23 (2024) 4349–4357. https://doi.org/10.1111/jocd.16566

[33] B. Fırtın, H. Yenipazar, A. Saygun, N. Şahin-Yeşilcubuk, Encapsulation of chia seed oil with curcumin and investigation of release behaivour & antioxidant properties of microcapsules during in vitro digestion studies, Lwt. 134 (2020) 109947. https://doi.org/10.1016/j.lwt.2020.109947

[34] W.W. Nandayasa, Febriyenti & H. Lucida, Optimization and characterization of quercetin vitamin C Nano-Phytosome Formulation, Int. J. Appl. Pharm. 15 (2023) 51-55. https://dx.doi.org/10.22159/ijap.2023.v15s1.47507

[35] A.A. Shitole, N. Sharma, P. Giram, A. Khandwekar, M. Baruah, B. Garnaik et al., LHRH-conjugated, PEGylated, poly-lactide-co-glycolide nanocapsules for targeted delivery of combinational chemotherapeutic drugs Docetaxel and Quercetin for prostate cancer, Mater Sci Eng C. 114 (2020) 111035. https://doi.org/10.1016/j.msec.2020.111035

[36] R.Q. Cron, G. Goyal, W.W. Chatham, Cytokine storm syndrome, Annu Rev Med. 74 (2023) 321–337. https://doi.org/10.1146/annurev-med-042921-112837

[37] A. Saeedi-Boroujeni, M.R. Mahmoudian-Sani, Anti-inflammatory potential of Quercetin in COVID-19 Treatment, J. Inflamm. 18 (2021) 3. https://doi.org/10.1186/s12950-021-00268-6

[38] H.X. Zhang, Y.Y. Li, Z.J. Liu, J.F. Wang, Quercetin effectively improves LPS-induced intestinal inflammation, pyroptosis, and disruption of the barrier function through the TLR4/NF-κB/NLRP3 signaling pathway in vivo and in vitro, Food Nutr. Res. 66 (2022): 8948. http://dx.doi.org/10.29219/fnr